Identification of a Highly Luminescent Au22(SG)18 Nanocluster. JACS 2014

ARTICLE *in* JOURNAL OF THE AMERICAN CHEMICAL SOCIETY · JANUARY 2014

Impact Factor: 12.11 · DOI: 10.1021/ja411643u · Source: PubMed

7 AUTHORS, INCLUDING:

Yong Yu
Agency for Science, Technology and Research …
23 PUBLICATIONS **626** CITATIONS
SEE PROFILE

David Tai Leong
National University of Singapore
86 PUBLICATIONS **2,102** CITATIONS
SEE PROFILE

Jianping Xie
National University of Singapore
110 PUBLICATIONS **4,402** CITATIONS
SEE PROFILE

JACS
JOURNAL OF THE AMERICAN CHEMICAL SOCIETY
Communication
pubs.acs.org/JACS

Identification of a Highly Luminescent $Au_{22}(SG)_{18}$ Nanocluster

Yong Yu,[†] Zhentao Luo,[†] Daniel M. Chevrier,[‡] David Tai Leong,[†] Peng Zhang,*[,‡] De-en Jiang,*[,§] and Jianping Xie*[,†]

[†]Department of Chemical and Biomolecular Engineering, National University of Singapore, Singapore 119260
[‡]Department of Chemistry and Institute for Research in Materials, Dalhousie University, Halifax, Nova Scotia B3H 4R2, Canada
[§]Chemical Sciences Division, Oak Ridge National Laboratory, Oak Ridge, Tennessee 37831, United States

Supporting Information

ABSTRACT: The luminescence property of thiolated gold nanoclusters (Au NCs) is thought to involve the Au(I)-thiolate motifs on the NC surface; however, this hypothesis remains largely unexplored because of the lack of precise molecular composition and structural information of highly luminescent Au NCs. Here we report a new red-emitting thiolated Au NC, which has a precise molecular formula of $Au_{22}(SR)_{18}$ and exhibits intense luminescence. Interestingly, this new $Au_{22}(SR)_{18}$ species shows distinctively different absorption and emission features from the previously reported $Au_{22}(SR)_{16}$, $Au_{22}(SR)_{17}$, and $Au_{25}(SR)_{18}$. In stark contrast, $Au_{22}(SR)_{18}$ luminesces intensely at ~665 nm with a high quantum yield of ~8%, while the other three Au NCs show very weak luminescence. Our results indicate that the luminescence of $Au_{22}(SR)_{18}$ originates from the long Au(I)-thiolate motifs on the NC surface via the aggregation-induced emission pathway. Structure prediction by density functional theory suggests that $Au_{22}(SR)_{18}$ has two RS-[Au-SR]$_3$ and two RS-[Au-SR]$_4$ motifs, interlocked and capping on a prolate Au_8 core. This predicted structure is further verified experimentally by Au L_3-edge X-ray absorption fine structure analysis.

Thiolated Au nanoclusters (NCs) or $Au_n(SR)_m$[1] have drawn increasing interest in the research community because of their intriguing molecular-like properties, such as quantized charging[2] and strong luminescence.[3] Being ultrasmall (with core sizes below 2 nm), the physicochemical properties of $Au_n(SR)_m$ become highly sensitive to their atomic composition and configuration; only one Au atom or one thiolate ligand difference (the value of n and m) can lead to remarkable differences in their physicochemical properties. Here we exemplify such a paradigm by first identifying an unprecedented thiolated Au NC species with a precise molecular formula of $Au_{22}(SR)_{18}$. $Au_{22}(SR)_{18}$ has the same number of thiolates as the well-characterized $Au_{25}(SR)_{18}$[4] but with a different number of Au atoms in its core. Further, $Au_{22}(SR)_{18}$ has the same number of Au atoms as the previously reported $Au_{22}(SR)_{16}$[5] and $Au_{22}(SR)_{17}$[5] but with a different number of thiolates on the NC surface. Despite the similarities in composition, $Au_{22}(SR)_{18}$ shows an unexpectedly strong red emission under UV illumination, while the other three Au NCs luminesce very weakly.

The red-emitting $Au_{22}(SR)_{18}$ NC with its precise molecular formula provides a good opportunity for understanding unresolved luminescence fundamentals of thiolated Au NCs, such as the origin of the luminescence and the possible cluster structure of luminescent Au NCs. Most reported atomically precise $Au_n(SR)_m$ NCs showed very weak luminescence in visible to near-infrared (NIR) region with a typical quantum yield (QY) of <0.1%.[5,6] Recently, we contributed to the Au NC universe with the synthesis of a new class of luminescent thiolated Au NCs,[7] showing intense orange emission at ~610 nm with a high QY of ~15%. We systematically showed that the luminescence of such thiolated Au NCs was generated by the aggregation-induced emission (AIE) of Au(I)-thiolate complexes on the NC surface. We reasoned from these data that the highly luminescent thiolated Au NCs would adopt a distinctly different cluster structure (e.g., different Au(I)-thiolate motifs) from the weakly luminescent species. But the lack of an unambiguous molecular formula for those highly luminescent Au NCs identified previously greatly limits our understanding of the structure–property relationship responsible for the high luminescence of thiolated Au NCs.

This challenge is specifically addressed in the present work by identifying and rigorously characterizing a new red-emitting thiolated Au NC species, leading to a promising prediction of a novel and unusual motif structure of luminescent Au NCs. The red-emitting thiolated Au NCs were synthesized from a modified carbon monoxide (CO)-reduction method[8] using a natural thiol-containing tripeptide, glutathione or GSH, as the protecting agent. As shown in Figure 1a, the raw product was brownish in aqueous solution (inset, item 1) and emitted intense red luminescence under UV light (inset, item 2). The resulting photoemission spectrum (Figure 1a, red line) shows a main peak at 665 nm with a shoulder peak at ~800 nm. In addition, the raw product showed two excitation peaks at 450 and 520 nm in the visible region (Figure 1a, blue line), which correspond well to the two absorption peaks (450 and 515 nm) observed in its absorption spectrum (Figure 1a, black line).

The as-synthesized red-emitting Au NCs were further characterized by native polyacrylamide gel electrophoresis (PAGE, 30%). We have synthesized a family of GSH-protected Au NCs with different sizes by using a protocol reported by Negishi et al.[5] and used this $Au_n(SG)_m$ family as a reference in the PAGE separation. As shown in Figure 1b, lane I, at least 9 discrete

Received: November 15, 2013
Published: January 3, 2014

   dx.doi.org/10.1021/ja411643u | J. Am. Chem. Soc. 2014, 136, 1246–1249

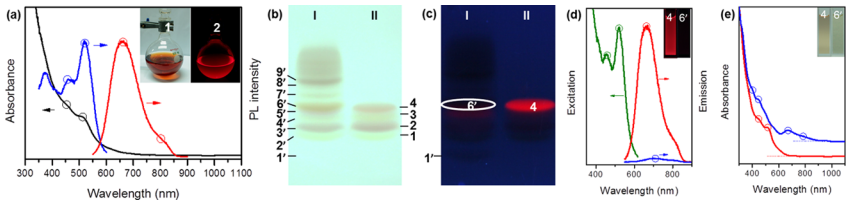

Figure 1. (a) UV−vis absorption (black line), photoemission (red line, λ_{ex} = 520 nm), and photoexcitation (blue line, λ_{em} = 665 nm) spectra of the raw red-emitting Au NCs. (Insets) Digital photos of the raw product dissolved in water under (1) visible and (2) UV light. (b and c) PAGE gels of (lane I) mix-sized $Au_n(SG)_m$ prepared according to a published protocol, and (lane II) the raw red-emitting Au NCs; under (b) visible and (c) UV light. (d) Photoemission spectra of **4** (red line) and **6′** (blue line) (λ_{ex} = 520 nm), and the photoexcitation spectrum of **4** (green line, λ_{em} = 665 nm). (Insets) Digital photos of **4** and **6′** under UV light. (e) UV−vis absorption spectra of **4** (red line) and **6′** (blue line). (Insets) Digital photos of **4** and **6′** under visible light.

bands have been identified, and they were labeled as bands **1′**−**9′** in the order of NC mobility (the size increases from band **1′** to **9′**). The color and optical property of each band were identical to those reported by Negishi et al.,[5] where bands **1′**−**9′** were determined to be $Au_{10-12}(SG)_{10-12}$, $Au_{15}(SG)_{13}$, $Au_{18}(SG)_{14}$, $Au_{22}(SG)_{16}$, $Au_{22}(SG)_{17}$, $Au_{25}(SG)_{18}$, $Au_{29}(SG)_{20}$, $Au_{33}(SG)_{22}$, and $Au_{38}(SG)_{24}$, respectively. In stark contrast, the PAGE analysis of the as-synthesized red-emitting Au NCs (Figure 1b, lane II) revealed only four closely spaced bands showing different colors, referring to bands **1**−**4** in the order of NC mobility. More interesting (though unexpected) observation is that only one band (**4**) showed strong red luminescence under UV light (Figure 1c, lane II), indicating that **4** was the only luminescent species in our raw product.

The mobility of band **4** was similar to that of band **6′** [$Au_{25}(SG)_{18}$] in the reference lane I, which suggests that species **4** and **6′** [$Au_{25}(SG)_{18}$] have a similar charge-to-mass ratio. However, **4** and **6′** showed distinctively different optical properties: **4** emitted intense red luminescence under UV light, while **6′** did not (Figure 1d, inset). In addition, the photoemission spectrum of **4** (Figure 1d, red line) was almost the same as that of the raw product (Figure 1a, red line), with a distinct peak at 665 nm. By comparison, **6′** only showed a weak luminescence at ∼700 nm (Figure 1d, blue line). The QY of **4** and **6′** calibrated with Rhodamine 6G were ∼8 and ∼0.2%, respectively. The photoexcitation spectrum of **4** (Figure 1d, green line) also resembled that of the raw product, further indicating that the red luminescence of the raw product was contributed predominantly by **4**. The solution color and absorption spectra of **4** and **6′** were also distinctly different. The absorption spectrum of **4** (Figure 1e, red line) showed two obvious peaks at 450 and 515 nm, while the absorption spectrum of **6′** (Figure 1e, blue line) showed four distinct peaks at 400, 445, 670, and 780 nm, which are the characteristic absorption of $Au_{25}(SG)_{18}$.[8a] Taken together, the PAGE and spectroscopic analysis suggest that **4** had a similar size as $Au_{25}(SG)_{18}$ but possessed distinctively different optical properties.

Electrospray ionization mass spectrometry (ESI-MS)[9] was then used to determine the molecular formula of **4**. As shown in Figure 2b (top panel), only one set of intense peaks at m/z ∼1970 is present in the m/z 1200−3000 range. The base peak (peak ***#1***) was at m/z 1968.47 in the resulting zoomed-in spectrum (middle panel). Isotope pattern analysis of the 1968.47 peak is shown in the bottom panel of Figure 2b (black (experimental) and red (simulated) line), indicating that the ionized NCs carried five units of negative charge (isotope peak spacing = 0.2). Hence, the molecular weight of the NCs was 9842.35 Da (1968.47 × 5), which is consistent with the molecular formula of $[Au_{22}(SG)_{18}{}^0 - 5H]^{5-}$ (molecular weight

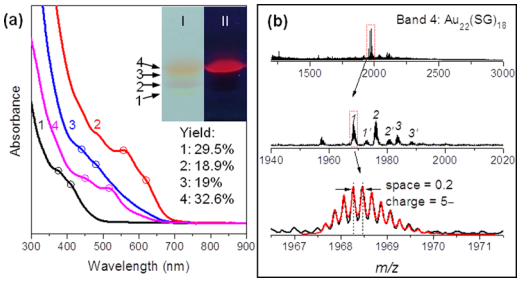

Figure 2. (a) UV−vis absorption spectra of Au NCs separated from bands **1**−**4** in the native PAGE gel (insets). (b) ESI mass spectra of species **4**. The red lines are the simulated isotope pattern of $[Au_{22}(SG)_{18}{}^0 - 5H]^{5-}$.

of 9841.6 Da). The above base peak was accompanied by two series of similar-looking but less-intense peaks (set ***a***: ***#2*** and ***#3***; set ***b***: ***#1′***−***#3′***, Figure 2b, middle panel), which could also be assigned as $Au_{22}(SG)_{18}$ carrying the same charge but with different proportions of adducts (Figure S1, Supporting Information (SI)).

The newly identified $Au_{22}(SG)_{18}$ has three Au atoms less than $Au_{25}(SG)_{18}$, but they have the same number of thiolate ligands (m = 18), which could be the reason for their similar mobility in the PAGE gel (Figure 1b). The new $Au_{22}(SG)_{18}$ species is also different from two previously reported Au_{22} species, $Au_{22}(SG)_{16}$ and $Au_{22}(SG)_{17}$. For example, $Au_{22}(SG)_{16}$ and $Au_{22}(SG)_{17}$ showed a distinct absorption peak at 560 and 540 nm, respectively, and both NCs emitted very weak luminescence with an emission wavelength at ∼720 nm and a low QY of <0.5%.[5] The absorption peak of $Au_{22}(SG)_{18}$ was further blue-shifted to 515 nm (Figure 1e, red line) compared to that of $Au_{22}(SG)_{16}$ and $Au_{22}(SG)_{17}$. Such a blue-shift in the absorption was also consistent with the trend observed in $Au_{22}(SG)_{16}$ and $Au_{22}(SG)_{17}$, where an obvious blue-shift of ∼20 nm was observed for $Au_{22}(SG)_{17}$ compared to $Au_{22}(SG)_{16}$.

The other three smaller Au NC species (bands **1**−**3**) in the raw product were also characterized by UV−vis absorption and ESI mass spectra. As shown in lane I of Figure 2a (or lane II of Figure 1b), band **1** appeared yellow in the PAGE gel and it shared the same mobility as band **2′** [$Au_{15}(SG)_{13}$] in lane I of Figure 1a. The absorption spectrum of band **1** (Figure 2a, black line) showed two distinct peaks at 375 and 410 nm, which corresponded well with the characteristic absorption of $Au_{15}(SG)_{13}$.[8c,10] ESI mass spectra of band **1** (Figure S2 (SI)) confirmed its formula of $Au_{15}(SG)_{13}$. Similarly, band **2** appeared murky green in the PAGE gel (Figure 2a, lane I, or Figure 1b, lane II), and it had the same mobility as band **3′** [$Au_{18}(SG)_{14}$] in lane I of Figure 1b. Band **2** showed two absorption features at 560 and 620 nm

dx.doi.org/10.1021/ja411643u | J. Am. Chem. Soc. 2014, 136, 1246−1249

(Figure 2a, red line), which are characteristic absorptions of $Au_{18}(SG)_{14}$.[8c,10] ESI mass spectra (Figure S3 (SI)) also confirmed its formula of $Au_{18}(SG)_{14}$. Band **3** has a NC size between $Au_{18}(SG)_{14}$ and $Au_{22}(SG)_{18}$ (Figure 1b, lane II or Figure 2a, lane I). Its absorption spectrum (Figure 2a, blue line) showed two distinct peaks at 440 and 480 nm, but we failed to determine its molecular formula by using ESI mass spectrometry. Taken together from the ESI-MS analysis, the raw product synthesized via the CO-reduction method was a NC mixture of four different sizes (**1**−**4**), among which only $Au_{22}(SG)_{18}$ (**4**) showed strong red emission under UV light. In addition, $Au_{22}(SG)_{18}$ was also the dominant NC species in the raw product with a typical yield of ∼32.6% based on the amount of Au atoms in the starting precursors according to inductively coupled plasma mass spectrometry (ICP-MS) measurements (inset of Figure 2a).

The molecular composition of $Au_{22}(SG)_{18}$ reflects its high content of thiolates on the NC surface. The thiolate-to-Au or SR/Au ratio of $Au_{22}(SG)_{18}$ was 0.82, which was also supported by X-ray photoelectron spectroscopy (XPS) analysis. As shown in Figure S4 (SI), the Au $4f_{7/2}$ binding energies of $Au_{22}(SG)_{18}$ (black line) were intermediate between those of Au(0) foil (red line) and Au(I)-SG complexes (blue line). Further deconvolution of the Au $4f_{7/2}$ spectrum into Au(0) and Au(I) components, with a binding energy of 83.9 and 84.3 eV, respectively, determined ∼67% Au(I) component of all Au atoms in $Au_{22}(SG)_{18}$. Luminescence lifetime measurements provided another line of evidence for the predominance of Au(I) component in $Au_{22}(SG)_{18}$. Analysis of the luminescence decay profile (Figure S5 (SI)) revealed that the microsecond lifetime components (1.37 μs (57.4%) and 0.46 μs (35.4%)) were predominant in $Au_{22}(SG)_{18}$. These values were also similar to the lifetimes of the reported orange-emitting Au NCs (Table S1 (SI)) with the aggregation-induced emission (AIE) feature.[7] Taken together, the high content of thiolates (∼0.82), the large Stokes shift (145 nm), and the microsecond-scale lifetime suggest that the emission from the atomically precise $Au_{22}(SG)_{18}$ was also derived from the AIE of Au(I)-thiolate complexes on the NC surface, similar to that reported in the orange-emitting Au(0)@Au(I)-thiolate NCs.

The determination of the unambiguous formula of the red-emitting $Au_{22}(SG)_{18}$ is the major contribution of this study. The precise molecular composition of $Au_{22}(SG)_{18}$ provides a key piece of information to predict the geometric structure of luminescent Au NCs, with the help from detailed analyses of the reported structures of thiolated Au NCs in both experimental and theoretical studies. The key hypothesis for structure prediction of thiolated Au NCs is that a $Au_n(SR)_m$ cluster has a gold core protected by $[RS(AuSR)]_x$ motifs and that clusters with higher SR/Au ratios (m/n) need longer staples (or greater x).[11] Recently solved structures of $Au_{102}(SR)_{44}$,[12] $Au_{25}(SR)_{18}$,[4b,d] $Au_{38}(SR)_{24}$,[13] and others[14] all showed this core-staple construction (see Table S2 (SI) for a summary of their structures).

Similarly, the staple hypothesis can be applied to predict the structure of $Au_{22}(SG)_{18}$. Table S2 (SI) also includes all possible combinations of Au(0) core and staple motifs for $Au_{22}(SR)_{18}$. Compared to $Au_{25}(SR)_{18}$, $Au_{22}(SR)_{18}$ has a higher SR/Au ratio (0.82 vs 0.72), and it should adopt a cluster structure with a smaller Au(0) core and several relatively longer motifs. In addition, $Au_{22}(SR)_{18}$ forms a nice sequence with three previously indentified clusters by a progressive difference of $Au_2(SR)_2$: $Au_{18}(SR)_{14}$,[15] $Au_{20}(SR)_{16}$,[11c,d] $Au_{24}(SR)_{20}$.[16] The SR/Au ratios of these four thiolated Au NCs were similar (∼0.80), and they all adopt the same $4e^-$ electron shell configuration. This configuration is also consistent with the anisotropic manner of the Au_8 core according to the superatom model.[17] From the above analyses, we conclude that the most reasonable strucure for $Au_{22}(SR)_{18}$ is a Au_8 core protected by two trimeric and two tetrameric staple motifs; in other words, $Au_{22}(SR)_{18} = Au_8 + 2[RS(AuSR)_3] + 2[RS(AuSR)_4]$. Given this construction, density functional theory (DFT) was then used to predict the most stable isomer of $Au_{22}(SG)_{18}$. Twelve isomers were explored, and the most stable isomer is shown in Figure 3a.

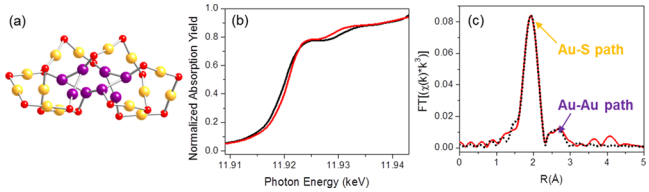

Figure 3. (a) The ball stick structure model of $Au_{22}(SR)_{18}$ predicted by DFT. The purple balls represent the eight Au atoms in the core, and the yellow balls represent the Au atoms in the staple motifs, while the red balls represent S atoms. All other atoms (carbon, hydrogen) have been omitted for clarity. (b) Au L_3-edge XANES spectra of $Au_{22}(SG)_{18}$ (red line) and Au foil (black line). (c) Experimental (red solid line) Au L_3-edge FT-EXAFS spectrum of $Au_{22}(SG)_{18}$ and the best fit (black dotted line).

Like $Au_{18}(SR)_{14}$,[15] $Au_{20}(SR)_{16}$,[11c,d] and $Au_{24}(SR)_{20}$,[16] it has a prolate Au_8 core. In addition, its four staple motifs can be divided into two groups, each of which consists of one trimer (RS-[Au-SR]$_3$) motif and one tetramer (RS-[Au-SR]$_4$) motif intercatenated. This interlocked configuration is a common feature of $Au_n(SR)_m$ clusters with high SR/Au ratios, such as $Au_{24}(SR)_{20}$[16] and $Au_{15}(SR)_{13}$.[18] DFT analysis of relative stability (Table S3 (SI)) indicates that this model of $Au_{22}(SR)_{18}$ is significantly more stable than the optimized models of $Au_{18}(SR)_{14}$ and $Au_{20}(SR)_{16}$, though slightly less stable than that of $Au_{24}(SR)_{20}$. The computed optical absorption spectrum for this model of $Au_{22}(SR)_{18}$ also shows reasonable agreement with the experimental one (Figure S6 (SI)).

X-ray absorption fine structure (XAFS) was then used to further probe the electronic structure and local environment of $Au_{22}(SG)_{18}$. As shown in Figure 3b, the X-ray absorption near-edge structure (XANES) spectrum of $Au_{22}(SG)_{18}$ (red line) shows a shift in the absorption edge to higher energy and a slightly more intense white-line compared to a Au foil reference (Figure 3b, black line), indicating a significant contribution of Au(I) electronic character, consistent with the Au(I)/Au(0) composition determined from XPS (Figure S4 (SI)). The extended X-ray absorption fine structure (EXAFS) spectrum was fitted to quantitatively examine the Au local structure (Figure 3c). Both Au−S and Au−Au scattering paths were used to fit the experimental data with results tabulated in Table S4 (SI). First, the Au−S CN value of 1.7 obtained from EXAFS fitting is in good agreement with the predicted model (Figure 3a), which has 8 Au bonded to 1 S (purple atoms) and 14 Au bonded to 2 S (yellow atoms), leading to a theoretical Au−S CN of 1.64. The Au−S bonding length of 2.314(4) Å from EXAFS (Table S4 (SI)) is also typically observed for Au(I)-thiolate semiring structures.[19] The local structure of $Au_{22}(SG)_{18}$ was further compared to that of the well-studied $Au_{25}(SR)_{18}$ (Figure S7 (SI)).[4d,19] A higher frequency of Au−S bonding and lower contribution from Au−Au core bonding was observed for $Au_{22}(SG)_{18}$, which corroborate

dx.doi.org/10.1021/ja411643u | J. Am. Chem. Soc. 2014, 136, 1246−1249

the longer Au(I)-thiolate motifs and smaller core in $Au_{22}(SG)_{18}$ (Figure 3a).

The predicted isomer was further confirmed by inspecting the site-specific Au−Au bonding with EXAFS. Examining the site-specific bonding environments with EXAFS is useful to verify the most stable structural isomer predicted by DFT calculations, since the Au−Au bonding environment in different structural isomers varies considerably. From the EXAFS fitting results, a very short Au−Au bond length of 2.67(1) Å has been identified and can be attributed to the unique Au_8 core structure. A close inspection of the DFT-predicted model (Figure 3a) points to a theoretical Au−Au CN of 0.64 when considering the number of Au−Au bonds in the Au_8 core that are much shorter than a typical face-centered cubic (fcc) Au−Au bond length (<2.88 Å). This theoretical value is also in good agreement with the first-shell Au−Au CN value of 0.7 obtained from our experimental EXAFS result.

In conclusion, a red-emitting thiolated Au nanocluster was discovered, and it has a precise composition of $Au_{22}(SG)_{18}$ identified by isotope-resolved ESI-MS. This newly identified $Au_{22}(SG)_{18}$ cluster showed unique absorption peaks at 450 and 515 nm and, more interestingly, emitted intense red luminescence at 665 nm with a high QY of ∼8%. Such optical properties were distinctively different from its neighboring NCs, including $Au_{22}(SG)_{16}$, $Au_{22}(SG)_{17}$, and $Au_{25}(SG)_{18}$. In addition, $Au_{22}(SG)_{18}$ features with a high SR/Au ratio (0.82), a large Stokes shift (145 nm), and a predominant microsecond-scale lifetime, which strongly suggest that the luminescence of $Au_{22}(SG)_{18}$ was originated from the AIE of the long motifs on the NC surface. A core-staple structure consisting of a prolate Au_8 core protected by two pairs of interlocked RS-$[Au\text{-}SR]_3$ and RS-$[Au\text{-}SR]_4$ motifs was predicted for $Au_{22}(SG)_{18}$ by DFT and further supported by experimental EXAFS analyses. The strong luminescence, the precise composition, the proposed structure of long motifs coupled with the Au_8 core, and the local bonding from the EXAFS analyses, afforded by the present discovery of $Au_{22}(SG)_{18}$, now provide important hints to understand the luminescent properties of thiolated Au NCs in aqueous solution.

■ ASSOCIATED CONTENT

Ⓢ Supporting Information

Experimental details and characterization data. This material is available free of charge via the Internet at http://pubs.acs.org.

■ AUTHOR INFORMATION

Corresponding Author

chexiej@nus.edu.sg; peng.zhang@dal.ca; jiangd@ornl.gov

Notes

The authors declare no competing financial interest.

■ ACKNOWLEDGMENTS

This work is financially supported by the Ministry of Education, Singapore, under Grants R-279-000-327-112. Work at ORNL was supported by the Division of Chemical Sciences, Geosciences, and Biosciences, Office of Basic Energy Sciences, U.S. Department of Energy.

■ REFERENCES

(1) (a) Jin, R. *Nanoscale* **2010**, *2*, 343. (b) Lu, Y.; Chen, W. *Chem. Soc. Rev.* **2012**, *41*, 3594. (c) Yu, Y.; Yao, Q.; Luo, Z.; Yuan, X.; Lee, J. Y.; Xie, J. *Nanoscale* **2013**, *5*, 4606.

(2) (a) Laaksonen, T.; Ruiz, V.; Liljeroth, P.; Quinn, B. M. *Chem. Soc. Rev.* **2008**, *37*, 1836. (b) Tang, Z.; Robinson, D. A.; Bokossa, N.; Xu, B.; Wang, S.; Wang, G. *J. Am. Chem. Soc.* **2011**, *133*, 16037. (c) Murray, R. W. *Chem. Rev.* **2008**, *108*, 2688.

(3) (a) Zhou, C.; Sun, C.; Yu, M.; Qin, Y.; Wang, J.; Kim, M.; Zheng, J. *J. Phys. Chem. C* **2010**, *114*, 7727. (b) Lin, C. A. J.; Yang, T. Y.; Lee, C. H.; Huang, S. H.; Sperling, R. A.; Zanella, M.; Li, J. K.; Shen, J. L.; Wang, H. H.; Yeh, H. I.; Parak, W. J.; Chang, W. H. *ACS Nano* **2009**, *3*, 395.

(4) (a) Dharmaratne, A. C.; Krick, T.; Dass, A. *J. Am. Chem. Soc.* **2009**, *131*, 13604. (b) Heaven, M. W.; Dass, A.; White, P. S.; Holt, K. M.; Murray, R. W. *J. Am. Chem. Soc.* **2008**, *130*, 3754. (c) Parker, J. F.; Fields-Zinna, C. A.; Murray, R. W. *Acc. Chem. Res.* **2010**, *43*, 1289. (d) Zhu, M.; Lanni, E.; Garg, N.; Bier, M. E.; Jin, R. *J. Am. Chem. Soc.* **2008**, *130*, 1138. (e) Shivhare, A.; Chevrier, D. M.; Purves, R. W.; Scott, R. W. J. *J. Phys. Chem. C* **2013**, *117*, 20007. (f) Cao, T.; Jin, S.; Wang, S.; Zhang, D.; Meng, X.; Zhu, M. *Nanoscale* **2013**, *5*, 7589.

(5) Negishi, Y.; Nobusada, K.; Tsukuda, T. *J. Am. Chem. Soc.* **2005**, *127*, 5261.

(6) (a) Link, S.; Beeby, A.; FitzGerald, S.; El-Sayed, M. A.; Schaaff, T. G.; Whetten, R. L. *J. Phys. Chem. B* **2002**, *106*, 3410. (b) Huang, T.; Murray, R. W. *J. Phys. Chem. B* **2001**, *105*, 12498. (c) Aldeek, F.; Muhammed, M. A. H.; Palui, G.; Zhan, N.; Mattoussi, H. *ACS Nano* **2013**, *7*, 2509.

(7) Luo, Z.; Yuan, X.; Yu, Y.; Zhang, Q.; Leong, D. T.; Lee, J. Y.; Xie, J. *J. Am. Chem. Soc.* **2012**, *134*, 16662.

(8) (a) Yu, Y.; Luo, Z.; Yu, Y.; Lee, J. Y.; Xie, J. *ACS Nano* **2012**, *6*, 7920. (b) Yu, Y.; Luo, Z.; Teo, C. S.; Tan, Y. N.; Xie, J. *Chem. Commun.* **2013**, *49*, 9740. (c) Yu, Y.; Chen, X.; Yao, Q.; Yu, Y.; Yan, N.; Xie, J. *Chem. Mater.* **2013**, *25*, 946.

(9) (a) Tracy, J. B.; Crowe, M. C.; Parker, J. F.; Hampe, O.; Fields-Zinna, C. A.; Dass, A.; Murray, R. W. *J. Am. Chem. Soc.* **2007**, *129*, 16209. (b) Tracy, J. B.; Kalyuzhny, G.; Crowe, M. C.; Balasubramanian, R.; Choi, J. P.; Murray, R. W. *J. Am. Chem. Soc.* **2007**, *129*, 6706.

(10) Yao, Q.; Yu, Y.; Yuan, X.; Yu, Y.; Xie, J.; Lee, J. Y. *Small* **2013**, *9*, 2696.

(11) (a) Jiang, D. E.; Tiago, M. L.; Luo, W.; Dai, S. *J. Am. Chem. Soc.* **2008**, *130*, 2777. (b) Chaki, N. K.; Negishi, Y.; Tsunoyama, H.; Shichibu, Y.; Tsukuda, T. *J. Am. Chem. Soc.* **2008**, *130*, 8608. (c) Jiang, D. E.; Chen, W.; Whetten, R. L.; Chen, Z. *J. Phys. Chem. C* **2009**, *113*, 16983. (d) Pei, Y.; Gao, Y.; Shao, N.; Zeng, X. C. *J. Am. Chem. Soc.* **2009**, *131*, 13619. (e) Nishigaki, J. I.; Tsunoyama, R.; Tsunoyama, H.; Ichikuni, N.; Yamazoe, S.; Negishi, Y.; Ito, M.; Matsuo, T.; Tamao, K.; Tsukuda, T. *J. Am. Chem. Soc.* **2012**, *134*, 14295. (f) Pei, Y.; Gao, Y.; Zeng, X. C. *J. Am. Chem. Soc.* **2008**, *130*, 7830.

(12) Jadzinsky, P. D.; Calero, G.; Ackerson, C. J.; Bushnell, D. A.; Kornberg, R. D. *Science* **2007**, *318*, 430.

(13) Qian, H.; Eckenhoff, W. T.; Zhu, Y.; Pintauer, T.; Jin, R. *J. Am. Chem. Soc.* **2010**, *132*, 8280.

(14) (a) Zeng, C.; Qian, H.; Li, T.; Li, G.; Rosi, N. L.; Yoon, B.; Barnett, R. N.; Whetten, R. L.; Landman, U.; Jin, R. *Angew. Chem., Int. Ed.* **2012**, *51*, 13114. (b) Zeng, C.; Li, T.; Das, A.; Rosi, N. L.; Jin, R. *J. Am. Chem. Soc.* **2013**, *135*, 10011.

(15) Tlahuice, A.; Garzon, I. L. *Phys. Chem. Chem. Phys.* **2012**, *14*, 3737.

(16) Pei, Y.; Pal, R.; Liu, C.; Gao, Y.; Zhang, Z.; Zeng, X. C. *J. Am. Chem. Soc.* **2012**, *134*, 3015.

(17) (a) Walter, M.; Akola, J.; Lopez-Acevedo, O.; Jadzinsky, P. D.; Calero, G.; Ackerson, C. J.; Whetten, R. L.; Grönbeck, H.; Häkkinen, H. *Proc. Natl. Acad. Sci. U. S. A.* **2008**, *105*, 9157. (b) Aikens, C. M. *J. Phys. Chem. Lett.* **2010**, *2*, 99. (c) Tofanelli, M. A.; Ackerson, C. J. *J. Am. Chem. Soc.* **2012**, *134*, 16937.

(18) Jiang, D. E.; Overbury, S. H.; Dai, S. *J. Am. Chem. Soc.* **2013**, *135*, 8786.

(19) (a) MacDonald, M. A.; Chevrier, D. M.; Zhang, P.; Qian, H.; Jin, R. *J. Phys. Chem. C* **2011**, *115*, 15282. (b) Chevrier, D. M.; MacDonald, M. A.; Chatt, A.; Zhang, P.; Wu, Z.; Jin, R. *J. Phys. Chem. C* **2012**, *116*, 25137.